Monatshefte für Chemie 138, 687–697 (2007)
DOI 10.1007/s00706-007-0652-z
Printed in The Netherlands

Monatshefte für Chemie
Chemical Monthly

Amphiphilic Dipyrrinones

Sanjeev K. Dey and **David A. Lightner***

Department of Chemistry, University of Nevada, Reno, Nevada, USA

Received January 17, 2007; accepted January 26, 2007; published online May 11, 2007

Summary. Replacing the typical lactam β-alkyl substituents of xanthobilirubinic acid and kryptopyrromethenone, two bilirubin analogs long used as model compounds in studies of its photochemistry and metabolism, leads to increased amphiphilicity. Synthesized by base-catalyzed condensation of 3,4-dimethoxypyrrolin-2-one with the appropriate pyrrole α-aldehyde, the 2,3-dimethoxyl analogs of xanthobilirubinic acid and kryptopyrromethenone are yellow-colored dipyrrinones that form intermolecular hydrogen-bonded dimers in the solid, as determined by X-ray crystallography, and in $CHCl_3$, as revealed by ^1H NMR and vapor pressure osmometry. These two new dipyrrinones are approximately ten times more soluble in water than their parent dipyrrinones.

Keywords. Pyrrole; Synthesis; X-Ray crystallography; Aqueous solubility

Introduction

Bilirubin (Fig. 1A), the yellow pigment of jaundice and the end product of heme metabolism [1] is known to have very poor aqueous solubility, with K_{sp} in *pH* 7 water at 37°C estimated to be $\sim 4 \times 10^{-15}\,M$ [2]. It is solubilized and transported in the circulation (blood) as a complex, non-covalently bound to serum albumin. In the liver the pigment's two propionic acids are esterified to mono- and diglucuronide esters [1], which are excreted into bile. A ridge-tile conformation of bilirubin [2–4], with its propionic acids tucked inward and firmly hydrogen bonded to opposing dipyrrinones (Fig. 1B) offers an explanation for the pigment's poor aqueous solubility [5]. Analogs of bilirubin, especially xanthobilirubinic acid (**3**) [6, 7] have been used to study photochemistry [8] and metabolism [7a]. Xanthobilirubinic (*XBR*, Fig. 1D) cannot engage in intramolecular hydrogen bonding yet is still very insoluble in water. Interest in improving the aqueous solubility of bilirubin, and thereby facilitating its elimination has led to syntheses of bilirubinoid analogs such as those having α-fluoro or α-methyl groups [9] in the propionic acid chains (which greatly lowers the pigment's pK_a), analogs substituted with ionized groups ionized groups ($-SO_3{}^-Na^+$) at C-10 [10], and a bilirubin pegylated at the *exo*-vinyl group [8–11]. Although the aqueous solubility was improved, the α-fluoro-rubin was completely soluble in water but also completely ionized to its carboxylate anions; the C(10) sulfonate group improved the pigment's aqueous solubility but again introduced an ionic center; and while the pegylated rubin was soluble in both water and $CHCl_3$, it was present as an aggregate in water presumably with bilirubin molecules aggregated inside a polyether micelle.

Seeking to retain the unmodified essential propionic acids while introducing no ionic groups and also seeking to avoid aggregation, we turned our attention to other potential structural modifications and found that *Merz et al.* [12] and *Wie et al.* [13] had counteracted the intrinsic aqueous *in*solubility of porphyrins by attaching short polyether chains, *e.g.*, diethylene glycol, at the pyrrole β-positions. Would replacing some of the pyrrole β-substituents of bilirubin produce a similar salutary effect and improve the pigment's aqueous solubility? And by how much? We considered the feasibility of synthesizing dipyrrinones and bilirubinoids with di- or triethylene

* Corresponding author. E-mail: lightner@scs.unr.edu

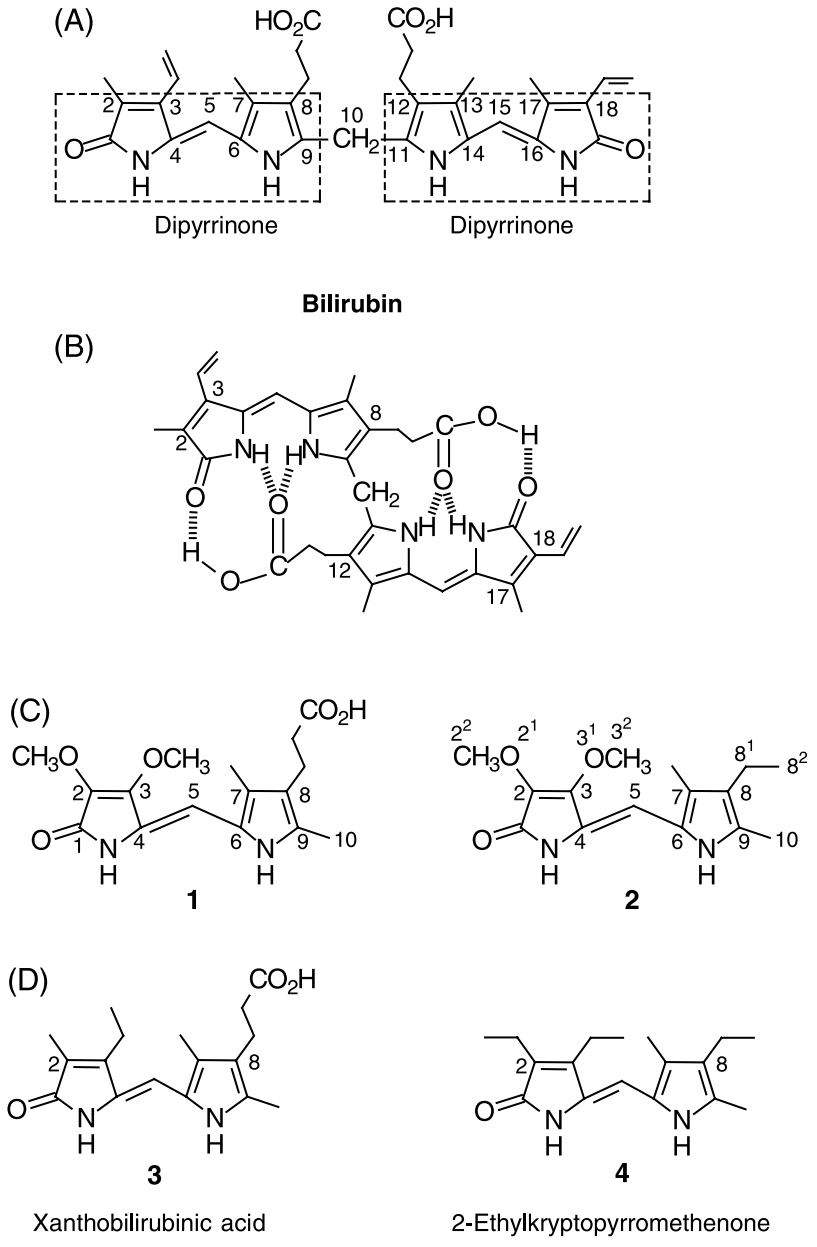

Fig. 1. (A) Bilirubin, composed of two dipyrrinones, stretched into a linear shape and (B) folded into a structure with six intramolecular hydrogen bonds. (C) The target 2,3-dimethoxydipyrrinones of this work. (D) Dipyrrinone analogs of bilirubin found useful in elucidating its photochemistry and photooxidation

glycol β-substituents while also questioning whether even the smallest β-ether (OCH_3) substituent might improve the aqueous solubility. In order to explore the possibility that replacing a few of the pyrrole β-substituents with methoxy groups might enhance the pigment's aqueous solubility – and to determine by how much, we synthesized two new dipyrrinones as test cases: **1**, an analog of *XBR* (**3**) and **2**, an analog of kryptopyrromethenone, both with two methoxy groups on the lactam rings (Fig. 1C). We report their syntheses herein and compare their properties relative to *XBR* (**3**) and the kryptopyrromethenone analog (**4**) with ethyl groups on the lactam ring (Fig. 1D).

Results and Discussion

Synthesis Aspects

Our approach to the syntheses of **1** and **2** followed the convention [2, 4] of condensing the appropriate

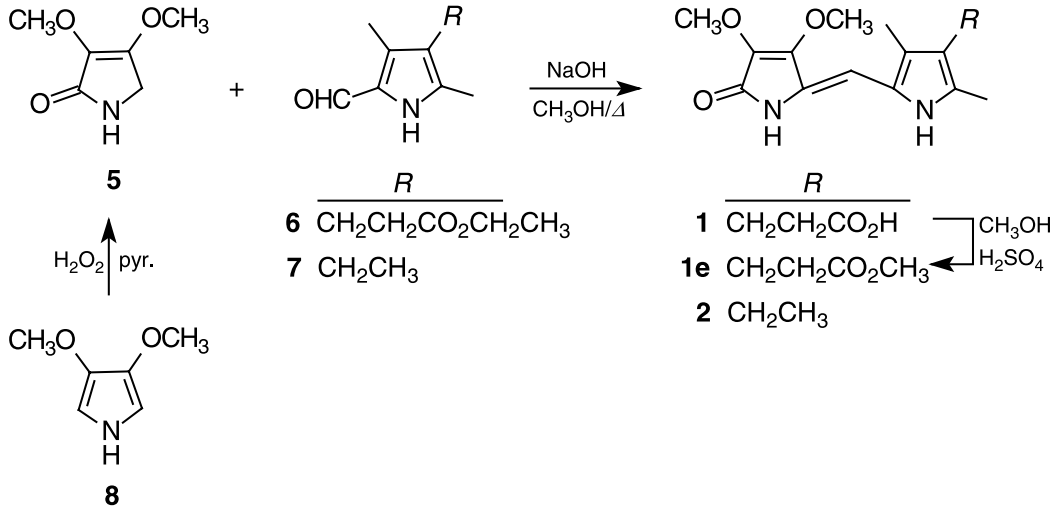

Scheme 1

pyrrole α-aldehyde, either **6** or **7** (Scheme 1) and 2,3-dimethoxypyrrolin-2-one (**5**). The pyrrole aldehydes were known from previous studies: 3,5-dimethyl-4-ethyl-2-formyl-(1*H*)-pyrrole (**7**) [14] from *Vilsmeier* formylation of kryptopyrrole [15], and 4-(2-carboethoxyethyl)-3,5-dimethyl-2-formyl-(1*H*)-pyrrole (**6**) [16] from treatment of the 2-carbo-*tert*-butoxy precursor [17] with trifluoroacetic acid and triethyl orthoformate. Dimethoxypyrrolinone **5** [18] was prepared by a simpler route in 81% yield by treating the known 3,4-dimethoxy-(1*H*)-pyrrole (**8**) [19] with 30% hydrogen peroxide in hot pyridine – a procedure developed earlier for converting 3,4-dialkyl pyrroles to their pyrrolinones [3]. 3,4-Dimethoxy-(1*H*)-pyrrole (**8**) was synthesized according to a literature procedure of *Merz* and *Meyer* [19]. Reaction of either **6** or **7** with excess **5** in hot methanolic potassium hydroxide led to the formation of yellow dipyrrinones **1** and **2** as solids. In order to prepare the methyl ester (**1e**) of **1**, the latter was submitted to *Fischer* esterification, and the desired ester was obtained in 83% yield.

Table 1. Comparison of the ^{13}C NMR chemical shifts (δ/ppm) of dimethoxydipyrrinones **1** and **2** with xanthobilirubinic acid (**3**) and 2-ethylkryptopyrromethenone (**4**) in $(CD_3)_2SO$ solvent

	Carbon[a]	**1**	**2**	**3**[b]	**4**
1	C=O	165.9	165.9	171.5	171.9
2	–C=	125.9	125.8	122.6	126.9
3	–C=	146.4	146.4	147.2	146.7
4	–C=	119.6	119.3	127.3	128.3
5	–CH=	96.6	96.7	97.6	97.9
6	–C=	121.2	121.8	121.7	121.8
7	–C=	122.0	121.0	122.3	122.0
8	–C=	118.6	121.7	118.7	121.6
9	–C=	129.4	128.7	129.4	128.7
2^1	CH_2/CH_3	–	–	8.1	17.0
2^2	CH_3	60.2	60.2	–	13.9
3^1	CH_2/CH_3	–	–	17.2	16.9
3^2	CH_3	59.0	59.0	14.8	13.9
7^1	CH_3	9.1	9.1	9.2	9.2
8^1	CH_2	19.4	16.9	19.5	17.0
8^2	CH_2/CH_3	35.0	15.5	35.0	15.8
8^3	CO_2H	174.0	–	174.0	–
10^1	CH_3	11.0	10.9	11.0	10.9

[a] For carbon numbering system, see Fig. 1
[b] Ref. [7a]

Structures and NMR Spectroscopy

The constitutional structures of **1** and **2** follow from the method of synthesis and comparison of their ^{13}C NMR spectral data with those of the known analogs **3** and **4** (Table 1). Methoxy carbons of **1** and **2** appear in the expected range; however, as expected from model systems differences in chemical shifts at C-2 and C-3 are not profound; however, the lactam carbonyls of **1** and **2** are shifted 5–6 ppm upfield, and C-4 is shifted 8–9 ppm upfield, both relative to **3** and **4**. Other carbon chemical shifts of **1** and **2** are similar to those of **3** and **4**, and the presence of OCH_3 groups on the lactam rings of **1** and **2** are fully evident from the CH_3 chemical shifts near 60 ppm.

The structure assignments are also consistent with the ^1H NMR spectra, from which one learns, in addi-

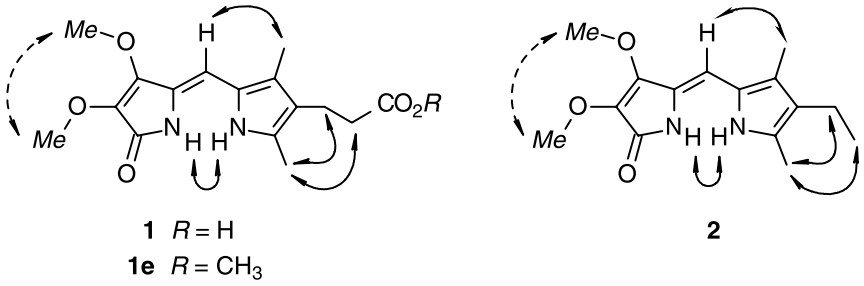

Fig. 2. Nuclear *Overhauser* effects observed and shown by curved arrows that confirm a *syn-Z* conformation in **1**, **1e**, and **2** in $(CD_3)_2SO$

Table 2. Comparison of the ^1H NMR N–H chemical shifts of dipyrrinones **1**–**4** in $CDCl_3$ and $(CD_3)_2SO$[a]

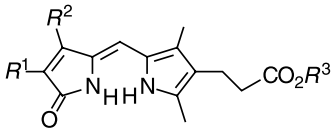

	R^1	R^2	R^3
1	OCH_3	OCH_3	H
1e	OCH_3	OCH_3	CH_3
3	CH_3	CH_2CH_3	H
3e	CH_3	CH_2CH_3	CH_3

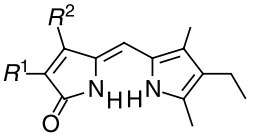

2: $R = OCH_3$
4: $R = CH_2CH_3$

	1	**1e**	**3**	**3e**	**2**	**4**
$CDCl_3$						
Lactam NH	insol.	10.61	insol.	11.15	10.43	11.14
Pyrrole NH	insol.	9.90	insol.	10.25	9.83	10.26
$(CD_3)_2SO$						
Lactam NH	9.54	9.60	9.67	9.72	9.54	9.72
Pyrrole NH	10.19	10.21	10.18	10.26	10.15	10.23

[a] Chemical shifts in δ/ppm downfield from $(CH_3)_4Si$ at 22°C

tion, that the favored pigment conformation is *syn-Z* (Fig. 2), as deduced from nuclear *Overhauser* spectroscopic (N*O*E) measurements. Thus in **1** and **2** (as well as **1e**, **3**, **3e**, and **4**) in $(CD_3)_2SO$ solvent one sees N*O*Es between the pyrrole lactam and NH hydrogens, and between the C(5)-H and the flanking groups at C(3) and C(7).

Dipyrrinones are typically monomeric in $(CD_3)_2SO$, with NH hydrogen bonding to solvent [3] and lactam and pyrrole NH chemical shifts near 9.6 and 10.3 ppm, respectively (Table 2) in the ^1H NMR spectra [13]. In contrast, in $CDCl_3$ intermolecularly hydrogen-bonded dimers are favored, as indicated by greater deshielding of the lactam NH resonance to ~11 ppm and only small changes in the pyrrole NH chemical shift. However, the NH chemical shifts in $CDCl_3$ (Table 2) seen for methoxy dipyrrinones **1e** and **2** do not exhibit as pronounced a deshielding as their analogs **3e** and **4**, and the pyrrole NH chemical shifts of **1e** and **2** are 0.3–0.4 ppm more shielded than **3e** and **4**. Whether such mismatches in chemical shifts were simply due to the electronic effects

Table 3. Molecular weights (*MW*s) of dipyrrinones **1e**, **2**, **3e**, and **4** determined by vapor pressure osmometry[a] at 45°C in $CHCl_3$

Compound	Formula weight (*FW*)/ g mol^{-1}	Measured weight (*MW*)/ g mol^{-1}
1e	334	670 ± 59
2	276	553 ± 10
3e	316	579 ± 20
4	272	544 ± 16

[a] Calibrated with benzil ($FW = 210$ g mol^{-1}, found $MW = 210 \pm 15$ g mol^{-1}); molecular weight in g mol^{-1}; conc. range, $1.1–7.0 \times 10^{-3}$ mol kg^{-1}

Table 4. Concentration dependence of the pyrrole (*P*-NH) and lactam (*L*-NH) ^{1}H NMR chemical shifts (δ/ppm) of dipyrrinones **2** and **4** in $CDCl_3$

Concentration/ (*M*)	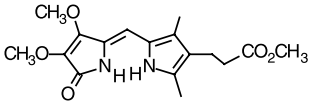 **1e**		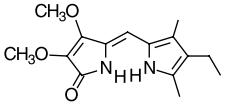 **2**		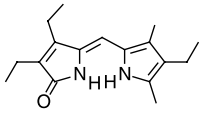 **4**	
	P-NH	*L*-NH	*P*-NH	*L*-NH	*P*-NH	*L*-NH
6.84×10^{-2}			10.01	10.81	10.40	11.35
1.53×10^{-2}	10.00	10.73	9.97	10.73	10.30	11.21
6.16×10^{-3}	9.95	10.64	9.88	10.58	10.28	11.17
3.42×10^{-3}	9.87	10.51	9.81	10.47	10.23	11.09
1.37×10^{-3}	9.82	10.42	9.68	10.22	10.11	10.93
8.1×10^{-4}	9.75	10.32	9.65	10.17	9.82	10.57
6.1×10^{-4}	9.73	10.24	9.59	10.07	9.84	10.50
4.5×10^{-4}	–	–	9.44	9.78	9.78	10.46
2.6×10^{-4}	9.53	9.90	–	–	–	–
1.8×10^{-4}	9.37	9.63	9.08	9.54	9.05	9.60
7.7×10^{-5}	8.98	8.98	8.98	8.98	–	–

of the methoxyl groups, or whether they were due to weaker intermolecular hydrogen bonding was initially unclear.

Vapor pressure osmometry (VPO) molecular weight measurements of **1e** and **2** in $CHCl_3$ (Table 3) confirmed that the methoxy dipyrrinones were dimers, as are **3e** and **4** within the concentration range $1–8 \times 10^{-3}\,M$. At high dilution, however, solutions of **3e** tend toward monomers, which exhibit extrapolated lactam and pyrrole NH chemical shifts of 7.00 and 7.75 ppm, respectively [20]. And as may be seen in Table 4, the pyrrole and lactam chemical shifts of **1e** and **2** move upfield as the pigment concentration decreases, with the lactam moving upfield faster. The behavior is qualitatively similar to that seen for **3e** and for kryptopyrromethenone [20] thus indicating only small differences in the ''tightness'' of the dimer hydrogen bonds between the methoxy and parent dipyrrinones and suggesting that differences in the chemical shifts found in the dimers are largely due to electronic perturbations by the methoxy groups.

Further support for the constitutional and conformational structures of **1e** and **2** comes from X-ray crystallography, which in addition confirms a *syn-Z* configuration for the dipyrrinones as well as intermolecular hydrogen bonding between pairs of dipyrrinones (Fig. 3). Thus, the presence of OCH_3 groups does not alter the configurational preference and preference for intermolecular hydrogen bonding established earlier for the alkyl analogs [3, 7, 21]. The influence of the methoxy groups on the lactam bond distances and angles is found to be only very small, and the dipyrrinone rings are essentially planar, as revealed by the torsion angles around C(5) as being near zero (Table 5). Unlike **4** [22] (or **1e**), the hydrogen-bonded dimer of **2** does not consist of two identical dipyrrinones but consists of similar but nonidentical molecules A and B. Nonetheless, the intermolecular hydrogen bonding distances remain very similar in **1e**, **2**, and **4**. The methoxy-dipyrrinones differ most noticeably from the reference parent (**4**) in the conformation of the lactam β-substituents relative to the lactam ring. In **4** the methyls at C(2^2) and C(3^2) are oriented approximately perpendicular to the lactam ring, $\sim +75°$ and $-86°$, respectively, one up and one down. In contrast, in **1e** and **2** only the C(2^2) methyl is oriented approximately perpendicular to the lactam ring (-75 to $-85°$) while the C(3^2) methyl lies only 15° out of the plane of the lactam ring and is oriented toward the C(2^1) oxygen. The intermolecularly hydrogen-bonded pairs of dipyrrinones, as in **1e** (Fig. 3) stack in columns (Fig. 4) with layers spaced apart by ~6.89 Å.

Optical Spectroscopy

The UV-Vis spectral data for **1**, **1e**, **2**, **3**, **3e**, and **4** in solvents with a wide range of polarity are given in Table 6. The long wavelength bands of **3**, **3e**, and **4** have nearly the same λ_{max} in the various solvents reported, as do **1**, **1e**, and **2**, with little variation from solvent to solvent, except in acetoni-

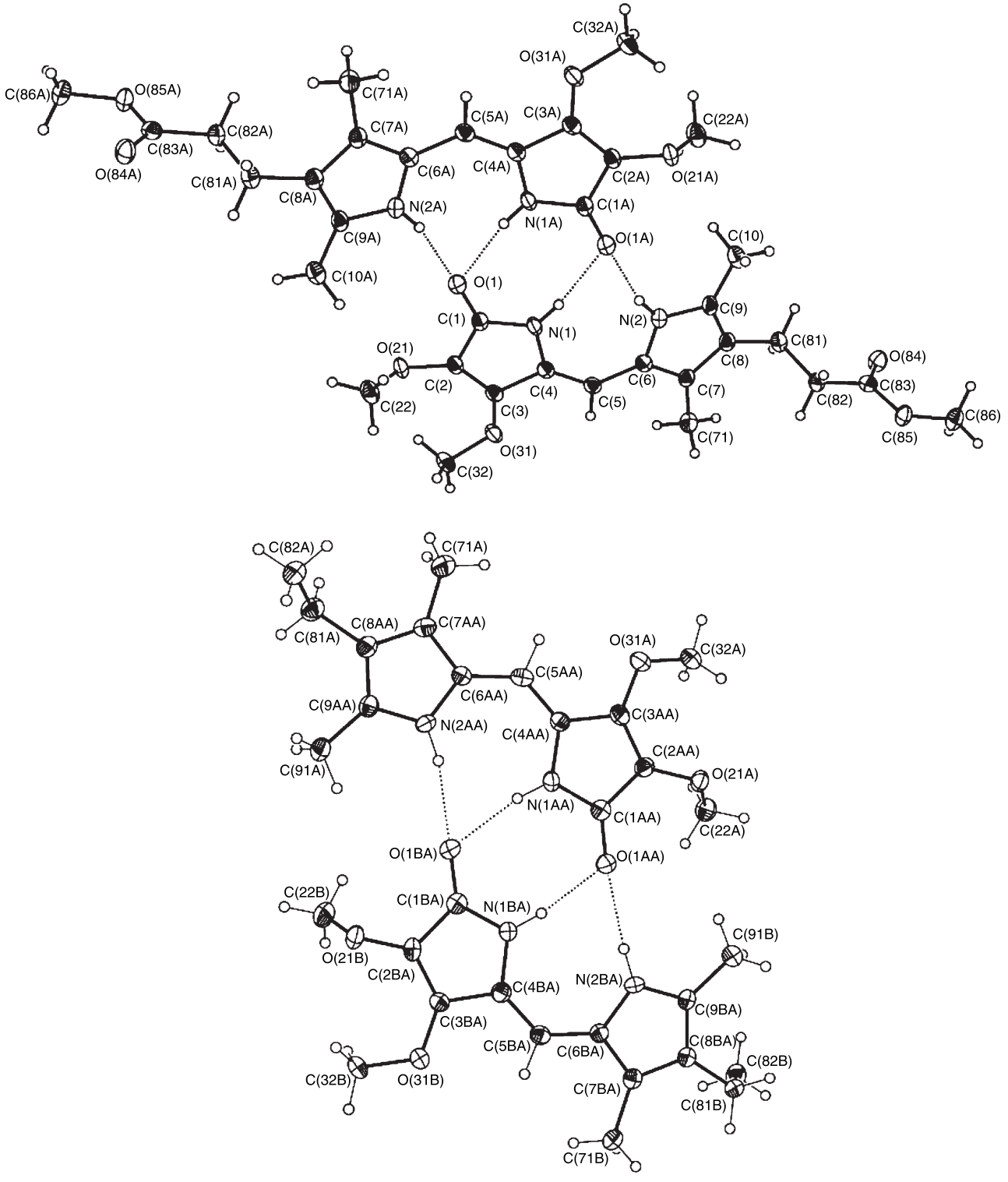

Fig. 3. Crystal structure drawings and numberings of **1e** (upper) and **2** (lower) showing intermolecular hydrogen bonding between the dipyrrinones; librational ellipsoids have been drawn with 50% probability

trile, where the λ_{max} are hypsochromically shifted. Most noteworthy is the observation that the presence of the methoxyl groups leads to a ~10–15 nm hypsochromic shift relative to the alkylated parents in each solvent studied – an indication of a strong electronic perturbation by directly-attached methoxyl

Table 5. Comparison of bond distances (d/Å) and torsion angles (ϕ/°) from the crystal structures of dipyrrinones **1e**, **2** (A and B molecules of the unit cell), and **4**

	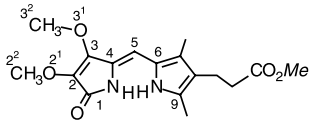 **1e**	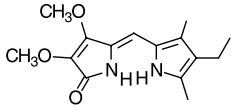 **2**		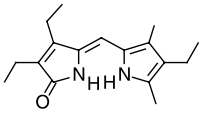 **4**
		A	B	
ϕ (2^2–2–2^1–1)	−84.7° (2)	−70.6° (3)	−75.5° (3)	+74.58° (19)
ϕ (3^2–3^1–3–4)	167.4° (16)	+162.0° (2)	+163.3° (2)	−86.0° (2)
ϕ (LN–4–5–6)	−4.0° (3)	−1.3 (5)	+0.2° (5)	0.3° (3)
ϕ (4–5–6–NP)	−3.2° (3)	+4.3° (5)	+9.7° (5)	−1.5° (3)
d (LNH · · · O=CL^1)	2.058	2.00[a]	1.97[a]	2.01[a]
d (LN to O=CL^1)	2.909	2.873 (3)	2.839 (3)	2.8713 (17)[a]
d (PNH · · · O=CL^1)	2.037	2.05[a]	2.05[a]	1.99 [a]
d (PN to O=CL^1)	2.880	2.920 (3)[a]	2.884 (3)[a]	2.8514 (17)[a]

[a] Distance between lactam (*L*) or pyrrole (*P*) of molecule A and molecule B

groups on the dipyrrinone long wavelength electronic transition.

Solubility

The characterization of dimethoxy-dipyrrinones **1**, **1e**, and **2** indicates the great similarity in solution and crystal structure and hydrogen bonding to the non-methoxylated parents: **3**, **3e**, and **4**. And while the dimethoxy analogs clearly behave like dipyrrinones, do they exhibit different solubility properties in water from the parents (which are very insoluble)? In order to investigate this aspect of behavior, we examined their aqueous solubility as well as their solubility in CH_3OH as a control. *UV*-visible spectroscopy was used to determine the concentrations relative to standard $\sim 1 \times 10^{-5}\,M$ solutions. The CH_3OH control experiment shows that the solubility of the pigment at $1\text{–}3 \times 10^{-5}\,M$ in pure CH_3OH is almost exactly the same as that in CH_3OH-2% $CHCl_3$ by volume, in which the pigment is freely soluble. All of the pigments are also freely soluble in a reference standard: H_2O-2% $(CH_3)_2SO$ by volume. Comparing pure H_2O to this reference (Table 7), one finds that the solubility of **1**, **1e**, and **2** are approximately ten times more soluble in water than **3**, **3e** and **4**, respectively, and that **1** and **1e** are approximately three times more soluble than **2**.

Concluding Comments

The presence of two methoxyl groups on the dipyrrinone lactam rings renders the pigment more soluble than the corresponding pigment with alkyl groups by a factor of approximately ten. When all four pyrrole β-substituents are methoxyl the aqueous solubility is improved by a factor of approximately two over the dimethoxydipyrrinones. Although the amphiphilicity is improved with methoxyl groups, complete aqueous solubility is more likely to arise with 2-methoxyethoxyl and 2-methoxyethoxyethoxyl groups and work is underway to prepare such substituted dipyrrinones as well as bilirubinoids with these β-substituents.

Experimental

NMR spectra were acquired on a Varian Unity Plus spectrometer at 11.75 T magnetic field strength operating at an ^{1}H frequency of 500 MHz and ^{13}C frequency of 125 MHz, or a Varian GE at 7.06 T magnetic field strength operating at an ^{1}H frequency of 300 MHz and a ^{13}C frequency of 75 MHz, in solutions of $CDCl_3$ (referenced at 7.26 ppm for ^{1}H and 77.23 ppm for ^{13}C) or $(CD_3)_2SO$ (referenced at 2.49 ppm for ^{1}H and 39.50 ppm for ^{13}C). The UV-Vis spectra were recorded on a Perkin-Elmer Lambda 12 spectrophotometer. Radial chromatography was carried out on Merck silica gel PF_{254} with $CaSO_4$ binder preparative layer grade, using a Chromatotron (Harrison Research, Inc., Palo Alto, CA) with 1, 2, or 4 mm thick rotors and analytical thin-layer chromatography was carried out on J.T. Baker silica gel IB-F plates (125 μm layer). Melting points were determined on a Mel-Temp capillary apparatus and are corrected. Satisfactory combustion analyses with experimental values within ±0.4% of theoretical for C, H and N were carried out by Desert Analytics, Tucson, AZ.

The spectral data were obtained in spectral grade solvents (Aldrich or Fisher). The starting compounds: 4-(2-carboxy-

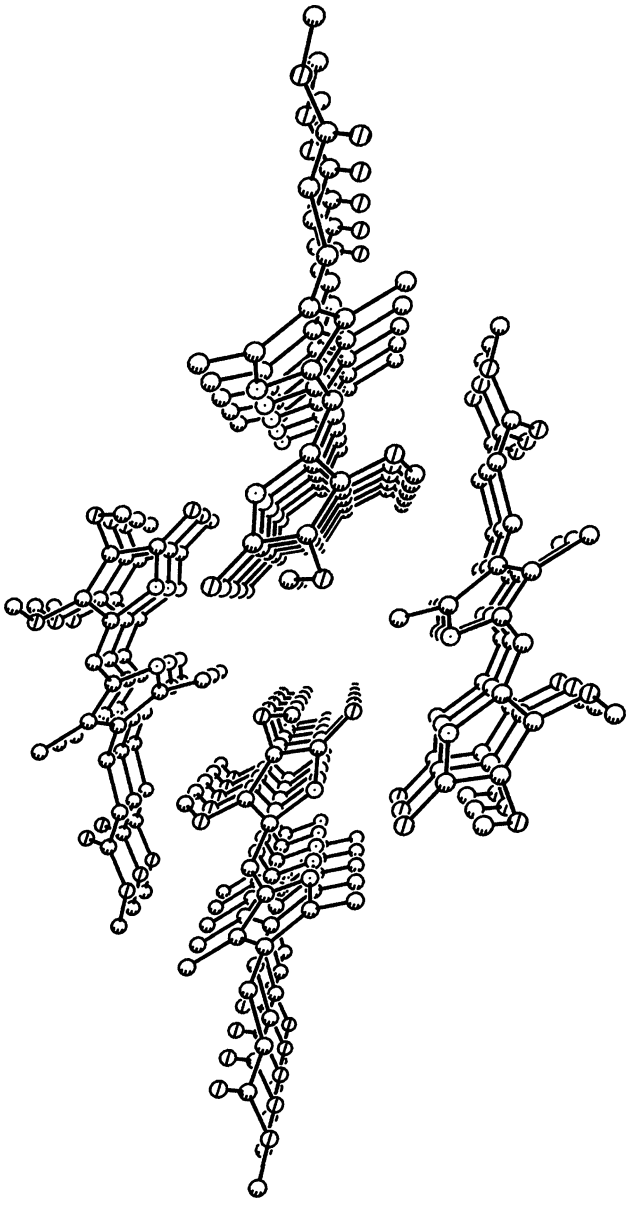

Fig. 4. Stacking pattern of intermolecularly hydrogen-bonded dyads of **1e**. (Hydrogen bonds are removed for clarity of representation.) Layers are stacked ~6.89 Å apart and a cross-section of the channel shown has approximate dimension 5.1 Å × 9.5 Å

ethyl)-3,5-dimethyl-2-formylpyrrole (**6**) [16], 3,5-dimethyl-4-ethyl-2-formylpyrrole (**7**) [14], and 3,4-dimethoxypyrrole (**8**) [19], xanthobilirubinic acid (**3**) and its methyl ester (**3e**) [7] and 2-ethylkryptopyrromethenone (**4**) [22] were synthesized according to literature methods.

Solubility in H_2O and CH_3OH

In order to compare the aqueous solubility of **1** *vs* **3**, **2** *vs* **4** and **1e** *vs* **3e**, stock solutions of each were prepared in $CHCl_3$ and in $(CH_3)_2SO$ solvents. Measured aliquots were withdrawn and diluted in 5.00 cm^3 volumetric flasks with CH_3OH or H_2O to create $\sim 1–3 \times 10^{-5}$ *M* pigment solutions in CH_3OH-2% $CHCl_3$ and in H_2O-2% $(CH_3)_2SO$. The UV-Vis absorbances of each were determined (~30000), and the solvent was removed to dryness. Then pure CH_3OH was added to the residue from evaporation of CH_3OH-2% $CHCl_3$ solutions, and pure H_2O (pH 7) was added to the residue from evaporation of the 10^{-5} *M* $CHCl_3$ solutions. After digestion by ultrasonication and centrifugation, the absorbances of the reconstituted CH_3OH and H_2O solutions were determined and compared with those of the original $\sim 1–3 \times 10^{-5}$ *M* solutions in order to determine the pigment concentrations.

8-(2-Carboxyethyl)-7,9-dimethyl-2,3-dimethoxy-(10H)-dipyrrinone (**1**, $C_{16}H_{20}N_2O_5$)

In a 100 cm^3 3 neck round bottom flask equipped with magnetic stirrer, condenser, N_2 inlet, and pyrrole aldehyde **6** [5b] (500 mg, 2.24 mmol) in 20 cm^3 CH_3OH was added 3,4-dimethoxypyrrolinone **5** (641 mg, 4.48 mmol) and 10 cm^3 5 *M* aqueous KOH solution. The resulting solution was heated at reflux for 72 h. The solvent was then evaporated (rotovap), and the resulting solid was dissolved in H_2O (10 cm^3), cooled in ice-bath and acidified, first few drops with conc. HNO_3 and then with dilute HNO_3 to reach *pH* **4**. The resulting yellow precipitate was collected by filtration and then taken up in cold CH_3OH, in which the pure acid **1** remained undissolved. The undissolved solid was recrystallized from CH_3OH–CH_2Cl_2 (1:1). Filtration and drying led to pure **1**. Yield: 360 mg (50%); mp 251–253°C (dec); ^{1}H NMR ($(CD_3)_2SO$, 500 MHz): $\delta = 1.97$ (s, 3H), 2.16 (s, 3H), 2.27 (t, $J = 7.2$ Hz, 2H), 2.54 (t, $J = 7.2$ Hz, 2H), 3.80 (s, 3H), 4.03 (s, 3H), 5.92 (s, 1H), 9.54 (s, 1H), 10.19 (s, 1H), 12.00 (s, 1H) ppm; ^{13}C NMR ($(CD_3)_2SO$, 125 MHz): $\delta = 9.1$, 11.0, 19.4, 35.0, 59.0, 60.2, 96.6, 118.6, 119.5, 121.2, 122.0, 125.9, 129.4, 146.4, 165.9, 174.0 ppm.

8-(2-Carbomethoxyethyl)-7,9-dimethyl-2,3-dimethoxy-(10H)-dipyrrin-2-one (**1e**, $C_{17}H_{18}N_2O_5$)

In a 500 cm^3 round bottom flask, equipped with magnetic stirrer, condenser, dipyrrinone **1** (200 mg, 6.25 mmol), and CH_3OH (200 cm^3) was added 25 cm^3 of 10% aqueous H_2SO_4, dropwise over 5 min. The resulting solution was heated at reflux and stirred for 1.5 h, after which the solvent was evaporated (rotovap) and the residual aqueous solution was extracted with dichloromethane to remove any yellow pigment completely from the aqueous layer. The combined organic layers were washed with saturated aqueous $NaHCO_3$ solution (2×100 cm^3 to extract unreacted acid, then dried over Na_2SO_4 (anhydrous) and evaporated (rotovap). The crude product was purified by radial chromatography (2% CH_3OH in CH_2Cl_2). The pure fraction was crystallized from CH_2Cl_2-hexane. Yield: 173 mg (83%); mp 209–210°C; ^{1}H NMR ($CDCl_3$, 500 MHz): $\delta = 2.04$ (s, 3H), 2.34 (s, 3H), 2.37 (t, $J = 7.2$ Hz, 2H), 2.65 (t, $J = 7.2$ Hz, 2H), 3.60 (s, 3H), 3.80 (s, 3H), 4.08 (s, 3H), 6.20 (s, 1H), 9.93 (br, s, 1H), 10.66 (br, s, 1H) ppm; ^{13}C NMR ($CDCl_3$, 125 MHz): $\delta = 9.7$, 11.5, 20.1, 35.3, 51.8, 59.3, 61.8, 101.0, 119.2, 119.2, 122.3, 125.1, 126.0, 132.0, 149,1, 168.6, 173.9 ppm.

Table 6. Comparison of solvent-dependence and influence of methoxyl groups on the UV-Vis spectral data of dipyrrinones **1**–**4**, **1e**, and **3e**

Pigment	λ_{max}/nm (ε/dm^3 mol^{-1} cm^{-1})[a]					
	C_6H_6	$CHCl_3$	CH_3CN	CH_3OH	$(CH_3)_2SO$	H_2O[b]
1	405 (24800)	402 (26300)	392 (30200)	403 (32900)	401 (34500)	403 (33000)
1e	400 (35200)	396 (31400)	390 (33400)	400 (35600)	400 (35600)	404 (17700)
2	402 (34900)	399 (30400)	392 (32200)	403 (35900)	402 (34700)	395 (14300) 439 (9100)[sh]
3	414 (28500)	411 (30100)	403 (27900)	414 (35000)	412 (32500)	412 (31500)
3e	413 (26500)	404 (34600)	402 (28900)	413 (38500)	412 (34800)	413 (19300)
4	412 (39900)	408 (35500)	406 (32000)	417 (40000)	416 (36500)	395 (15500) 454 (9500)[sh]

[a] Measured at 10^{-5} *M*; [b] contains 2% $(CH_3)_2SO$

Table 7. Comparison of the solubility of dipyrrinones in methanol and water

Dipyrrinone	Methanol[a] [Pigment]$_f$/[Pigment]	Water[b] [Pigment]$_f$/[Pigment]
Dimethoxy *XBR* **1**	(0.681/0.723) 0.99:1	(0.215/0.793) 0.27:1
Dimethoxy *XBR* methyl ester **1e**	(0.631/0.636) 1:1	(0.0893/0.292) 0.31:1
Dimethoxydipyrrinone **2**	(0.999/1.034) 0.94:1	(0.0283/0.337) 0.09:1
XBR **3**	(0.448/0.443) 1:1	(0.0250/0.419) 0.06:1
XBR methyl ester **3e**	(0.768/0.772) 1:1	(0.00883/0.388) 0.023:1
2-Ethylkryptopyrromethenone **4**	(1.044/1.113) 0.94:1	(0.00197/0.431) 0.005:1

[a] Ratio of pigment concentration in methanol solvent *vs* standard solution (2% $CHCl_3$ in CH_3OH) as compared by UV-Vis spectroscopy; [b] ratio of pigment concentration in H_2O *vs* standard solution (2% DMSO in H_2O), compared by UV-Vis spectroscopy. The standard solutions are prepared and ultrasonicated, the UV-Vis absorbance at λ_{max} is recorded. The solution is evaporated to dryness and then the pure solvent (CH_3OH or H_2O) is added, the solution/mixture is ultrasonicated, and the absorbance is remeasured. In all cases it is less than in the standard solutions. The ratio of absolute pigment concentrations is found in parentheses, the relative pigment concentrations are outside the parentheses. The methodology is found in the text

7,9-Dimethyl-2,3-dimethoxy-8-ethyl-(10H)-dipyrrin-2-one (**2**, $C_{15}H_{20}N_2O_3$)

In a 100 cm^3, 3 neck round bottom flask equipped with magnetic stirrer, condenser, N_2 inlet, and kryptopyrrole aldehyde **7** [14] (80 mg, 0.53 mmol) in 6 cm^3 CH_3OH was added 3,4-dimethoxypyrrolinone **5** (227 mg, 1.58 mmol eq.) and 2.5 cm^3 5 *M* aqueous NaOH. The resulting solution was heated at reflux for 24 h, and the reaction was cooled in an ice bath and acidified to give a brown-yellow solid, which was collected by suction filtration, washed with H_2O and dried with suction. After drying, the resulting solid was washed with cold CH_3OH, and the dissolved solid on the funnel turned out to be pure **2**, which was crystallized from CH_2Cl_2–CH_3OH to afford yellow crystals. Yield: 40 mg (27%); mp 246–247°C; ^{1}H NMR ($CDCl_3$, 500 MHz): $\delta =$ 1.06 (t, $J = 7.1$ Hz, 3H), 2.11 (s, 3H), 2.4 (s and q, 5H), 3.87 (s, 3H), 4.16 (s, 3H), 6.41 (s, 1H), 9.91 (br, s, 1H), 10.63 (br, s, 1H) ppm; ^{13}C NMR ($CDCl_3$, 125 MHz): $\delta = 10.1$, 11.81, 16.0, 18.0, 59.7, 62.1, 101.6, 119.2, 122.5, 123.5, 125.5, 126.5, 131.9, 149.5, 169.9 ppm.

3,4-Dimethoxypyrrolin-2-one (**5**, $C_6H_9NO_2$)

To a 100 cm^3 round bottom flask equipped with magnetic stirrer, condenser, N_2 inlet, was added 3,4-dimethoxypyrrole (**8**, 1.07 g, 8.4 mmol) and 8 cm^3 pyridine. To the resulting solution was added 30% H_2O_2 (1.5 cm^3) followed by 1.5 h reflux. The reaction was cooled, and the pyridine was removed (rotovap) by forming azeotropic mixture with toluene. After removal of the solvent, the crude solid was dissolved in CH_2Cl_2 and purified by column chromatography using 1% MeOH in CH_2Cl_2 eluent. Pure compound **3** was a yellow solid. Yield: 946 mg (81%); mp 72–75°C; ^{1}H NMR ($CDCl_3$, 300 MHz): $\delta = 3.78$ (d, $J = 1.4$ Hz, 2H), 3.86 (s, 3H), 4.03 (s, 3H), 5.38 (br, s, 1H) ppm; ^{13}C NMR ($CDCl_3$, 75 MHz): $\delta = 42.2$, 58.3, 60.2, 126.6, 152.9, 171.4 ppm.

X-Ray Structure and Solution

Crystals of **1e** and **2** were grown by slow diffusion of *n*-hexane into a solution of CH_2Cl_2. A crystal was placed into the tip of a 0.1 mm diameter glass capillary and mounted on a *Bruker* SMART Apex system for data collection at 100(2) K. A pre-

Table 8. Crystal data and structure refinement for **1e** and **2**

Compound	**1e**	**2**
Empirical formula	$C_{17}H_{22}N_2O_5$	$C_{15}H_{20}N_2O_3$
Formula weight	334.37	276.33
Temperature	273(2) K	273(2) K
Wavelength	0.71073 Å	0.71073 Å
Crystal system	Monoclinic	Monoclinic
Space group	$P2(1)/c$	$P2(1)/c$
Unit cell dimensions	$a = 17.7366(7)$ Å	$a = 14.8846(11)$ Å
	$b = 6.8910(3)$ Å	$b = 14.7311(11)$ Å
	$c = 13.5903(5)$ Å	$c = 12.8899(9)$ Å
	$\alpha = 90°$	$\alpha = 90°$
	$\delta = 97.911(3)°$	$\delta = 90.839(2)°$
	$\gamma = 90°$	$\gamma = 90°$
Volume	1645.24(11) Å^3	2826.0(4) Å^3
Z	4	8
Density (calculated)	1.350 Mg/m^3	1.299 Mg/m^3
Absorption coefficient	0.100 mm^{-1}	0.091 mm^{-1}
$F(000)$	712	1184
Crystal size	$0.95 \times 0.09 \times 0.06$ mm^3	$0.10 \times 0.08 \times 0.05$ mm^3
Theta range for data collection	1.16 to 27.49°	1.95 to 25.00°
Index ranges	$-22 \le h \le 22$, $-8 \le k \le 8$,	$-17 \le h \le 17$, $17 \le k \le 17$,
	$-17 \le l \le 17$	$-15 \le l \le 15$
Reflections collected	22082	29722
Independent reflections	3755 [R(int) = 0.0744]	4984 [R(int) = 0.1253]
Completeness to theta = 27.49° (**1e**)	99.7%	
Completeness to theta = 25.00° (**2**)		100.0%
Absorption correction	SADABS	SADABS
Max. and min. transmission	0.9937 and 0.9107	0.9957 and 0.9907
Refinement method	Full-matrix least-squares on $F2$	Full-matrix least-squares on $F2$
Data/restraints/parameters	3755/0/222	4984/0/371
Goodness-of-fit on $F2$	1.219	0.933
Final R indices [$I > 2$sigma(I)]	$R1 = 0.0436$, $wR2 = 0.0956$	$R1 = 0.0521$, $wR2 = 0.1124$
R indices (all data)	$R1 = 0.0945$, $wR2 = 0.1120$	$R1 = 0.1216$, $wR2 = 0.1294$
Largest diff. peak and hole	0.224 and −0.281 e.Å^{-3}	0.290 and −0.262 e.Å^{-3}

liminary set of cell constants was calculated from reflections harvested from 3 sets of 20 frames for **1e** and 3 sets of 20 frames for **2**. These initial sets of frames were oriented such that orthogonal wedges of reciprocal space were surveyed (final orientation matrices determined from global least-squares refinement of 4984 reflections for **2** and 3755 for **1e**). The data collection was carried out using MoKα radiation (0.71073 Å graphite monochromator) with a frame time of 20 s for **1e** and 20 s for **2** and a detector distance of 4.94 cm. A randomly oriented region of reciprocal space was surveyed to the extent of 2 hemispheres and to a resolution of 0.66 Å. Four major sections of frames were collected with 0.5° steps in ω at 600 different ϕ settings and a detector position of 27° in 2θ for **1e**. The intensity data were corrected for absorption and decay (SADABS) [23]. Final cell constants were calculated from the *xyz* centroids of strong reflections from the actual data collection after integration (SAINT 6.45, 2003) [24]. Crystal data and refinement information for **1e** and **2** may be found in Table 8.

The structure was solved and refined using SHELXL-L [25]. The monoclinic space group $P2(1)/c$ for **2** and monoclinic $P2(1)/c$ for **1e** were determined based on systematic absences and intensity statistics. A direct-methods solution was calculated which provided most non-hydrogen atoms from the *E*-map. Full-matrix least squares/difference *Fourier* cycles were performed for structure refinement. All non-hydrogen atoms were refined with anisotropic displacement parameters unless stated otherwise. Hydrogen atom positions were placed in ideal positions and refined as riding atoms with relative isotropic displacement parameters (a C–H distance fixed at 0.96 Å and a thermal parameter 1.2 times the host carbon atom). Tables of atomic coordinates, bond lengths and angles, anisotropic displacement parameters, hydrogen coordinates and isotropic displacement parameters have been deposited at the Cambridge Crystallographic Data Centre, CCDC No. 630872 for **1e** and 630871 for **2**.

Acknowledgements

We thank the U.S. National Institutes of Health (HD 17779) for generous support of this research. We also thank the National

Science Foundation (CHE-0226402) for providing funding to purchase the X-ray diffractometer used in this work. *SKD* is an *R.C. Fuson* graduate fellow.

References

[1] Chowdhury JH, Wolkoff AW, Chowdhury NR, Arias IM (2001) Hereditary Jaundice and Disorders of Bilirubin Metabolism. In: Scriver CF, Beaudet WS, Sly AL, Valle D (eds) The Metabolic and Molecular Bases of Inherited Disease, vol II. McGraw-Hill Inc., NY, chap 125, pp 3063–3101

[2] Bonnett R, Davies JE, Hursthouse NB, Sheldrick GM (1978) Proc R Soc London, Ser B **202**: 249

[3] Falk H (1989) The Chemistry of Linear Oligopyrroles and Bile Pigments. Springer-Verlag, Wien

[4] Person RV, Peterson BR, Lightner DA (1994) J Am Chem Soc **116**: 42

[5] Brodersen R (1982) Physical Chemistry of Bilirubin: Binding to Macromolecules and Membranes. In: Heirwegh KPM, Brown SB (eds) Bilirubin, vol I. CRC Press, Boca Raton, Florida, chap 3, p 76

[6] Boiadjiev SE, Lightner DA (2006) Org Prep Proc Intl **38**: 347

[7] (a) Boiadjiev SE, Conley BA, Brower JO, McDonagh AF, Lightner DA (2006) Monatsh Chem **137**: 1463; (b) Shrout DP, Lightner DA (1990) Synthesis 1062

[8] (a) Lightner DA, Park Y-T (1979) Tetrahedron **35**: 463; (b) Landen GL, Park Y-T, Lightner DA (1983) Tetrahedron **39**: 1893 (Symposium-in-Print on Linear Tetrapyrroles); (c) Lamola AA, Braslavsky SE, Schaffner K, Lightner DA (1983) Photochem Photobiol **37**: 263

[9] (a) Boiadjiev SE, Lightner DA (1997) J Org Chem **62**: 399; (b) Boiadjiev S, Lightner DA (1998) J Org Chem **63**: 6220

[10] Senge MO, Ma JS, McDonagh AF (2001) Bioorg Med Chem Lett **11**: 875

[11] Boiadjiev SE, Watters K, Lai B, Wolf S, Welch W, McDonagh AF, Lightner, DA (2004) Biochemistry **43**: 15617

[12] Merz A, Schroppe R, Dötterl (1995) Synthesis 795

[13] Wie W-H, Wang Z, Mizuno T, Cortez C, Fu L, Sirisawad M, Naumorski L, Magda D, Sessler JL (2006) Dalton Trans 1934

[14] (a) Lightner DA, Quistad GB (1972) Angew Chem **84**: 216; (b) Lightner DA, Quistad GB (1972) Angew Chem Int Ed Engl **11**: 215; (c) Lightner DA, Quistad GB (1973) J Heterocyclic Chem **10**: 273

[15] (a) Lightner DA, Crandall DC (1973) Experientia **29**: 262; (b) Shrout DP, Lightner DA (1990) Synthesis 1062

[16] Grigg R, Johnson AW, Kenyon R, Math VB, Richardson K (1969) J Chem Soc (C): 176

[17] Brower JO, Lightner DA, McDonagh AF (2000) Tetrahedron **56**: 7869

[18] Stachel HD, Porschenrieder H, Redlin J, Schachtner J, Zeitler K (1994) Liebig's Ann Chem 129

[19] Merz A, Meyer T (1999) Synthesis 94

[20] Nogales DF, Ma J-S, Lightner DA (1993) Tetrahedron **49**: 2361

[21] Huggins MT, Lightner DA (2001) Monatsh Chem **132**: 203

[22] Cullen DL, Black PS, Meyer EF, Lightner DA, Quistad GB, Pak C-S (1977) Tetrahedron **33**: 477

[23] Sheldrick GM (2003) SADABS, V6.14, Bruker Analytical X-ray Systems, Madison, WI, USA

[24] SAINT V6.45, Bruker Analytical X-ray Systems, Madison, WI, USA

[25] Sheldrick GM (2003) SHELXL-L V6.14, Bruker Analytical X-ray Systems, Madison, WI, USA